

*Samuel Stearns  
September 19, 1964*

HIGH ENERGY  $\gamma$  RAY SOURCE FROM ELECTRON POSITRON PAIR ANNIHILATION\*

Yung-Su Tsai

Stanford Linear Accelerator Center  
Stanford University, Stanford, California

ABSTRACT

Problems associated with using the process  $e^+ + e^- \rightarrow 2\gamma$  as a source for high energy  $\gamma$  ray are investigated. The polarization of the  $\gamma$ 's is shown to be negligible at high energies. The spread of  $\gamma$  spectra at a fixed angle due to radiative corrections is investigated. It was found that terms like  $\frac{\alpha}{\pi} \ln^2 \frac{4E^2}{m^2}$  are associated with infrared divergence and disappear with a reasonable energy resolution. The result obtained is found to be very similar to Schwinger's corrections without vacuum polarization. Our result was found to be also usable in the colliding beam experiment without any modification under certain conditions.

(To be submitted to Physical Review)

---

\*Work supported by U. S. Atomic Energy Commission.

## 1. INTRODUCTION

In the usual experiments involving photons as incident particles, the photon source is from the ordinary bremsstrahlungs which are not only non-monochromatic but also strongly dominated by low energy  $\gamma$ 's due to the  $1/k$  dependence in the bremsstrahlung cross sections. This fact not only imposes some complications to the kinematical analysis of the subsequent photoproduction processes but also sometimes renders the experiments impossible due to the enormous background produced by the low energy  $\gamma$ 's; for example in the bubble chamber experiments there will be too many compton electrons and electron pairs produced. Ballam and Guiragossian<sup>1</sup> made a proposal to use the fact that when positrons are injected into the hydrogen target one obtains monochromatic  $\gamma$ 's from  $e^+ + e^- \rightarrow 2\gamma$  process in addition to the ordinary bremsstrahlung from  $e^+ + e^- \rightarrow e^+ + e^- + \gamma$  and  $e^+ + p \rightarrow e^+ + p + \gamma$ . One hopes that the  $\gamma$ 's thus produced will have sufficiently high energy components to overcome part of the difficulties mentioned above. In order to obtain a resultant gamma spectra from  $e^+$  hydrogen atom collision one has to calculate the following four processes in detail:

1.  $e^+ + e^- \rightarrow 2\gamma$  and its radiative corrections
2.  $e^+ + e^- \rightarrow 3\gamma$
3.  $e^+ + e^- \rightarrow e^+ + e^- + \gamma$
4.  $e^+ + p \rightarrow e^+ + p + \gamma$

In this paper we treat only the 1st process and part of the second process where the third photon emitted is limited to a low energy. The exact treatments

of process 2, 3 and 4 can be done by an electronic computer and will be published separately.<sup>2</sup> Figure 1 shows the anticipated  $\gamma$  spectrum at a fixed angle. The spike in the figure is due to process 1 and 2. The processes 2, 3 and 4 contribute to the smooth curve in the background. The troublesome low energy end of the spectrum can usually be greatly reduced by passing the  $\gamma$  rays through some material using the fact that the absorption coefficient for the low energy  $\gamma$  rays is larger than that for the high energy  $\gamma$  rays.

In Section 2, we treat the lowest order process, define the notations, give many useful kinematical relations and formulae and show that the polarization of the  $\gamma$  rays produced in the process  $e^+ + e^- \rightarrow 2\gamma$  is negligibly small at high energies. In Section 3 the spreading of the  $\gamma$  spectra due to radiative corrections is calculated. It was found that the terms like  $\frac{\alpha}{\pi} \ln^2 \frac{4E^2}{m^2}$  do not occur in our final expression for the radiative corrections  $\delta$ . It is concluded that terms like  $\frac{\alpha}{\pi} \ln^2 \frac{4E^2}{m^2}$  are closely related to the infrared phenomena and disappear when the phase space for the third photon  $k_3$  is taken to be such that  $\omega_3^{\max} \gg m$  in the center of mass system. (See Section 5.) In Section 4 some numerical examples are given. In Section 5, the physical significance of existence or absence of terms like  $\frac{\alpha}{\pi} \ln^2 \frac{4E^2}{m^2}$  is discussed. The resemblance between our results and Schwinger's formula is pointed out, and finally the adaption of our result to the colliding beam experiment is considered. In the Appendix we discuss some precautions needed in the calculation of cross sections involving many identical particles in the final states.

2.  $e^+ + e^- \rightarrow 2\gamma$

In this section we treat the lowest order cross section. Since we are interested only in the very high energy  $e^+$  beam we may treat the electron in the hydrogen atom to be free.  $P_1$  and  $P_2$  represent the four momenta of the target electron and the incident positron respectively.  $k_1$  and  $e_1$  represent the four momenta and polarization vector of the detected photon and  $k_2$  and  $e_2$  represent those of the undetected photon. Quantities with a bar on top represent the center of mass quantities. Our metric is defined such that if  $k_1 = (\omega_1, \bar{k}_1)$  and  $P_1 = (E_1, \bar{P}_1)$ , then  $k_1 \cdot P_1 = \omega_1 E_1 - \bar{k}_1 \cdot \bar{P}_1$ . The units used are  $\frac{e^2}{4\pi} = \alpha$ , and  $\hbar = c = 1$ . We choose a gauge such that in the laboratory system ( $P_1 = (m, 0)$ ),  $e_1 \cdot P_1 = e_2 \cdot P_1 = 0$  and  $e_1 \cdot k_1 = e_2 \cdot k_2 = 0$ . By calculating the lowest order Feynman diagrams shown in Fig. 2, one obtains the differential cross section

$$\frac{d\sigma_0}{d\Omega_k}(e_1, e_2) = \frac{r_0^2}{8} \frac{m^2 (m + E_2)}{P_2 (m + E_2 - P_2 \cos\theta)^2} \left[ \frac{\omega_1}{\omega_2} + \frac{\omega_2}{\omega_1} + 2 - 4 (e_1 \cdot e_2)^2 \right] \dots \quad (2-1)$$

where  $r_0^2 = 7.95 \times 10^{-26} \text{ cm}^2$  and  $\theta$  is the angle between  $\bar{P}_2$  and  $\bar{k}_1$ .

For convenience in discussing the polarization, let us choose a coordinate in which the direction of  $\bar{k}_1$ , is the  $z$  axis and that of  $\bar{k}_1 \times \bar{k}_2$  is the  $y$  axis as shown in Fig. 3. Then the summation over  $e_2$  can be carried out with respect to two transverse directions

$$e_{2\parallel} \equiv (0, +\cos\theta_{12}, 0, -\sin\theta_{12})$$

$$e_{2\perp} \equiv (0, 0, 1, 0)$$

and the result is

$$\frac{d\sigma_o}{d\Omega_{k_1}} (e_1) = \frac{A}{2} \left\{ \frac{\omega_1}{\omega_2} + \frac{\omega_2}{\omega_1} + 2 - 2 \left( e_{1x}^2 \cos^2\theta_{12} + e_{1y}^2 \right) \right\} \quad (2-2)$$

where

$$A \equiv \frac{r_o^2}{2} \frac{m^2 (m + E_2)}{P_2 (m + E_2 - P_2 \cos\theta)^2}$$

From Eq. (2-2) we can construct the density matrix for the photon beam  $k_1$ ,

$$X_{ij} = \frac{A}{2} \left\{ \left( \frac{\omega_1}{\omega_2} + \frac{\omega_2}{\omega_1} + 2 \right) \delta_{ij} - 2 \left( \delta_{ix} \delta_{jx} \cos^2\theta_{12} + \delta_{iy} \delta_{jy} \right) \right\} \quad (2-3)$$

where  $i = x, y$  and  $j = x, y$ .

The density matrix  $X$  completely specifies the quantum mechanical description of a monochromatic photon beam  $k_1$  because any subsequent interaction of  $k_1$  can be written as  $\text{Tr} MXM^\dagger$  where  $M$  is the matrix element of the subsequent interaction. (Provided one uses the same gauge as used here.)

However it is more convenient to give an equivalent description in terms of intensity of the beam and the three Stokes parameters  $S_x, S_y,$  and  $S_z$ .

The trace of  $X$  gives the differential cross section summed over the polarization  $e_1$  and is given by

$$\frac{d\sigma_o}{d\Omega_{k_1}} = \text{Tr} X = A \left\{ \frac{\omega_1}{\omega_2} + \frac{\omega_2}{\omega_1} + \sin^2\theta_{12} \right\} \quad (2-4)$$

The definitions of the Stokes parameters, their functional form of our particular problem and their physical meanings can be given by the following equations.<sup>3</sup> (See Fig. 4.)

$$S_x = \frac{\text{Tr } \sigma_x X}{\text{Tr } X} = \frac{X_{yx} + X_{xy}}{\text{Tr } X} = 0$$

$$= \frac{d\sigma \left( \hat{e}_1 = \frac{\hat{e}_x + \hat{e}_y}{\sqrt{2}} \right) - d\sigma \left( \hat{e}_1 = \frac{\hat{e}_x - \hat{e}_y}{\sqrt{2}} \right)}{d\sigma \left( \hat{e}_1 = \frac{\hat{e}_x + \hat{e}_y}{\sqrt{2}} \right) + d\sigma \left( \hat{e}_1 = \frac{\hat{e}_x - \hat{e}_y}{\sqrt{2}} \right)}$$
(2-5)

$$S_y = \frac{\text{Tr } \sigma_y X}{\text{Tr } X} = \frac{i(X_{xy} - X_{yx})}{\text{Tr } X} = 0$$

$$= \frac{d\sigma \left( \hat{e}_1 = \frac{\hat{e}_x - i\hat{e}_y}{\sqrt{2}} \right) - d\sigma \left( \hat{e}_1 = \frac{\hat{e}_x + i\hat{e}_y}{\sqrt{2}} \right)}{d\sigma \left( \hat{e}_1 = \frac{\hat{e}_x - i\hat{e}_y}{\sqrt{2}} \right) + d\sigma \left( \hat{e}_1 = \frac{\hat{e}_x + i\hat{e}_y}{\sqrt{2}} \right)}$$
(2-6)

$$S_z = \frac{\text{Tr } \sigma_z X}{\text{Tr } X} = \frac{X_{xx} - X_{yy}}{\text{Tr } X} = \frac{\sin^2 \theta_{12}}{\frac{\omega_1}{\omega_2} + \frac{\omega_2}{\omega_1} + \sin^2 \theta_{12}}$$

$$= \frac{d\sigma \left( \hat{e}_1 = \hat{e}_x \right) - d\sigma \left( \hat{e}_1 = \hat{e}_y \right)}{d\sigma \left( \hat{e}_1 = \hat{e}_x \right) + d\sigma \left( \hat{e}_1 = \hat{e}_y \right)}$$
(2-7)

It is seen that the only nonvanishing Stokes parameter is  $S_z$  and Eq. (2-7) shows that there are more photons plane polarized in the production plane (x-z plane) than those perpendicular to the production plane. The magnitude of  $S_z$  is roughly proportional to  $\theta_{12}^2$ , the square of the angle between two photons produced. The differential cross section and the only nonvanishing Stokes parameter  $S_z$  of Eqs. (2-4) and (2-7) can be written in terms of  $\theta$  and  $E_2$  alone by the following kinematic relations.

$$\omega_1 = \frac{(E_2 + m) m}{m + E_2 - P_2 \cos\theta} \approx \frac{E_2}{1 + \frac{\gamma\theta^2}{2}}, \quad (2-8)$$

$$\omega_2 = \frac{(E_2 + m) (E_2 - P_2 \cos\theta)}{m + E_2 - P_2 \cos\theta} \approx \frac{E_2 \frac{\gamma\theta^2}{2}}{1 + \frac{\gamma\theta^2}{2}}, \quad (2-9)$$

$$\sin^2\theta_{12} = \frac{2(E_2 - m) \sin^2\theta}{E_2 - P_2 \cos\theta} - \frac{(E_2 - m)^2 \sin^4\theta}{(E_2 - P_2 \cos\theta)^2} \approx \frac{4}{\gamma^2 \theta^2} \approx 0. \quad (2-10)$$

The approximate relations  $\approx$  hold only when

$$1 \gg \theta \gg \frac{m}{E_2} \equiv \frac{1}{\gamma}. \quad (2-11)$$

Hereafter we use the symbol  $\approx$  to represent approximate relations true only if inequalities Eq. (2-11) are satisfied.

When  $1 \gg \theta$  and  $\gamma \gg 1$  we may write<sup>4</sup>

$$\frac{d\sigma_o}{d\Omega_k} = \frac{r_o^2}{2} \frac{1}{\left[1 + \frac{\gamma\theta^2}{2}\right]^2} \left[ \frac{2\gamma}{1 + \gamma^2\theta^2} + \frac{1 + \gamma^2\theta^2}{2\gamma} + \frac{4\gamma^2\theta^2}{1 + \gamma^2\theta^2} - \frac{4\gamma^4\theta^4}{(1 + \gamma^2\theta^2)^2} \right] \quad (2-12)$$

$$\approx \frac{r_o^2}{2} \frac{1}{\left[1 + \frac{\gamma\theta^2}{2}\right]^2} \left( \frac{2}{\gamma\theta^2} + \frac{\gamma\theta^2}{2} \right) \quad (2-13)$$

The second relation holds only when inequalities Eq. (2-11) are satisfied.

Similarly for  $S_z$  we have

$$S_z = \frac{8\theta^2\gamma}{(4 + \gamma^2\theta^4)(1 + \gamma^2\theta^2)} \quad (2-14)$$

$$\approx 0$$

For convenience of order of magnitude estimate we give some of the values of  $d\sigma/d\Omega_{k_1}$  and  $S_z$  in Table I.

TABLE I

$\theta$	$\frac{d\sigma}{d\Omega_{k_1}}$	$S_z$
0	$r_o^2\gamma$	0
$\frac{1}{\gamma}$	$\frac{r_o^2\gamma}{2}$	$\frac{1}{\gamma}$
$\sqrt{\frac{1}{\gamma}}$	$\frac{5}{9} r_o^2$	$\frac{8}{5\gamma}$



### 3. RADIATIVE CORRECTIONS

From the experience in the electron scattering from nuclei, we know that the radiative corrections are quite important whenever one deals with interactions involving extremely relativistic charged particles. In our case the radiative corrections will induce a tail to the spike in Fig. 1, a phenomenon very similar to the radiative tails in the electron scatterings. Harris<sup>5</sup> and Brown have previously calculated the radiative corrections to the pair annihilation, assuming the maximum energy of the 3rd photon emitted,  $\omega_3^{\max}$ , to be isotropic in angle and  $\omega_3^{\max} \ll m$  in the laboratory frame. Their results were obtained by using the substitution rule on the earlier paper by Brown and Feynman<sup>6</sup> on Compton scattering. The calculation can be divided into two parts; the virtual radiative corrections represented by Fig. 5 and real radiative corrections represented by Fig. 6. The expressions for the virtual radiative corrections are independent of experimental conditions. Thus we use the results of HB for this part. The real radiative corrections have to be recalculated because the results depend upon the experimental set up. For convenience of calculation we shall use the center of mass system. We define  $\bar{E} = \bar{E}_1 = \bar{E}_2$ ,  $\bar{P} = (\bar{E}^2 - m^2)^{\frac{1}{2}}$  and  $\bar{\theta}$  to be the angle between  $\bar{P}_2$  and  $\bar{k}_1$ .

According to Harris and Brown the cross section for the  $e^+ + e^- \rightarrow 2\gamma$  up to order  $e^6$ , averaged over spins and summed over polarizations can be written as<sup>7</sup>

$$\frac{d\sigma_{2\gamma}}{d\Omega_{k_1}} = \frac{d\sigma_0}{d\Omega_{k_1}} \left\{ 1 - \frac{\alpha}{\pi} \left[ 2 (1 - 2x \coth 2x) \ln \frac{\lambda}{m} - 4x \coth 2x \left( 2g(x) - h(2x) + \frac{\pi^2}{4x} \right) + F(\kappa, \tau) + F(\tau, \kappa) \right] \right\} \quad (3-1)$$

where  $\lambda$  is the usual fictitious photon mass and

$$\begin{aligned}
 F(\kappa, \tau) u = & \left[ 4x (\kappa \tau)^{-1} \sinh 2x (1 + 2 \cosh^2 x) + 2x \tanh x \right] g(x) \\
 & + \ln \kappa \left\{ 4x \coth 2x \left[ \frac{4}{\kappa^2} - \frac{1}{\kappa} - \frac{\tau}{2\kappa} - 1 - 4 (\kappa \tau)^{-1} \sinh^2 x \right] \right. \\
 & - \frac{2x}{\sinh 2x} \left( \frac{\kappa - 6}{\tau} \right) + \frac{3\tau}{2\kappa^2} (1 + \kappa) + \frac{3}{\tau} + 1 - \frac{7}{\kappa\tau} + \frac{8}{\kappa} - \frac{8}{\kappa^2} - \frac{\tau^2 - 2\kappa + \kappa^2\tau}{2\kappa^2\tau (\kappa - 1)} \\
 & \left. - \frac{2\kappa^2 + \tau}{2\tau (\kappa - 1)^2} \right\} - \frac{\frac{1}{4} \pi^2 - x^2}{\cosh^2 x} \left\{ \frac{2}{\kappa} - \frac{7\kappa}{4} - \frac{3\tau^2}{4\kappa} \right\} - 4x \coth x \left\{ \frac{1}{2} - \frac{1}{\kappa} \right\} \\
 & + 4 \left( \frac{1}{\kappa} + \frac{1}{\tau} \right)^2 - \frac{12}{\kappa} - \frac{3\kappa}{2\tau} - \frac{2\kappa}{\tau^2} + \frac{1}{\kappa-1} \left( \frac{\kappa}{\tau} + \frac{1}{2} \right) \\
 & + G_0(\kappa) \left\{ \frac{\kappa^2}{\tau} + \frac{\tau}{\kappa^2} + \frac{\kappa}{\tau} + \kappa + \frac{\tau}{2} + \frac{2}{\kappa} - \frac{3}{\tau} - 1 \right\}. \tag{3-2}
 \end{aligned}$$

The symbols used in the above equations have the following meaning:

$$\kappa \equiv \frac{2P \cdot k}{m^2} = \frac{2P \cdot k}{m^2},$$

$$\tau \equiv \frac{2P \cdot k}{m^2} = \frac{2P \cdot k}{m^2},$$

$$\kappa + \tau = \frac{4\bar{E}^2}{m^2} \equiv 4\bar{\gamma}^2,$$

$$\cosh x = \bar{\gamma} = \sqrt{\frac{\gamma}{2}} ,$$

$$u = 4 \left( \frac{1}{\kappa} + \frac{1}{\tau} \right)^2 - 4 \left( \frac{1}{\kappa} + \frac{1}{\tau} \right) - \left( \frac{\kappa}{\tau} + \frac{\tau}{\kappa} \right) ,$$

$$g(x) = \frac{1}{x} \int_0^x u \tanh u \, du ,$$

$$h(x) = \frac{1}{x} \int_0^x u \coth u \, du ,$$

and

$$G_0(x) = \frac{2}{\kappa} \int_1^{1-\kappa} \ln(1-u) \frac{du}{u} .$$

We notice that if the inequalities (2-11) hold, then

$$\tau \gg \bar{\gamma} \gg 1 \quad (3-3a)$$

and

$$\kappa \gg \bar{\gamma} \gg 1 . \quad (3-3b)$$

Since the definitions given above by HB are unwieldy we give simplified (but exact) expressions as well as approximate expressions which hold only when (2-11) is satisfied.

$$u \approx - \left( \frac{\kappa}{\tau} + \frac{\tau}{\kappa} \right) ,$$

$$x = \frac{1}{2} \ln \frac{\bar{E} + \bar{P}}{\bar{E} - \bar{P}} \approx \ln 2\bar{\gamma} ,$$

$$\sinh x = \frac{\bar{P}}{m} \approx \bar{\gamma} ,$$

$$\cosh 2x = 2\bar{\gamma}^{-2} - 1 \approx 2\bar{\gamma}^{-2},$$

$$\sinh 2x = \frac{2\bar{E}\bar{P}}{m^2} \approx 2\bar{\gamma}^{-2},$$

$$g(x) = \ln 2\bar{\gamma} - \frac{x}{2} - \frac{\pi^2}{12x} - \frac{1}{2x} \Phi(-e^{-2x}) \approx \frac{x}{2},$$

$$h(x) = \ln(2\sinh x) - \frac{x}{2} - \frac{\pi^2}{12x} - \frac{1}{2x} \Phi(e^{-2x}) \approx \frac{x}{2},$$

$$G_0(\kappa) = \frac{-2}{\kappa} \left( \Phi(1-\kappa) - \Phi(1) \right) \approx \frac{1}{\kappa} \left( \ln^2 \kappa + \frac{2\pi^2}{3} \right),$$

where  $\Phi(x)$  is the Spence function defined as

$$\Phi(x) = - \int_0^x \frac{\ln|1-u|}{u} du.$$

Substituting the approximate expressions given above into Eq. (3-1) and neglecting terms small compared with 1 inside the bracket [ ] we obtain<sup>6</sup>

$$\frac{d\sigma_{2\gamma}}{d\Omega_{k_1}} \approx \frac{d\sigma_0}{d\Omega} \left\{ 1 - \frac{\alpha}{\pi} \left[ \left( 1 - \frac{\bar{E}^2 + \bar{P}^2}{2\bar{E}\bar{P}} \ln \frac{\bar{E} + \bar{P}}{\bar{E} - \bar{P}} \right) \left( \frac{3}{2} + 2\ln \frac{\lambda}{m} \right) + 2\ln^2 2\bar{\gamma} - \frac{\pi^2}{6} + f \right] \right\} \quad (3-4)$$

where

$$\begin{aligned} fu = & \left( 1 + \frac{\kappa}{\tau} + \frac{\tau}{2\kappa} \right) \left\{ \ln^2 \frac{\kappa+\tau}{\kappa} + \ln \frac{\kappa}{\kappa+\tau} \right\} \\ & + \left( 1 + \frac{\tau}{\kappa} + \frac{\kappa}{2\tau} \right) \left\{ \ln^2 \frac{\kappa+\tau}{\tau} + \ln \frac{\tau}{\kappa+\tau} \right\} \\ & + \left( \frac{\tau}{\kappa} - \frac{\kappa}{\tau} \right) \ln \frac{\kappa}{\tau} + \pi^2 \left\{ \frac{1}{3} + \frac{1}{12} \left( \frac{\kappa}{\tau} + \frac{\tau}{\kappa} \right) \right\} \end{aligned} \quad (3-5)$$

We next calculate the cross section for  $e^+ + e^- \rightarrow 3\gamma$ . In principle one could calculate this cross section exactly by going into the center of mass system of two undetected particles as was done in other three particle final state problems.<sup>9</sup> We shall not calculate this cross section exactly here but merely try to find the dominant terms (such as  $\log \gamma$ ,  $\ln \gamma \ln \frac{\omega_1}{\Delta\omega_1}$  etc.), because these terms can be obtained without much effort and one expects that the resultant formula should be accurate to within one or two percent which is hopefully quite sufficient for the experimentalists needs. We shall calculate everything in the center of mass system.<sup>10</sup> To do this we have to specify what we are looking for in the laboratory system and then transform the lab experimental conditions into those of the C.M. We are interested in the photon spectra at a certain angle in the lab system. We anticipate the spectrum will look like what is shown in Fig. 7. (The photons due to ordinary bremsstrahlung have been subtracted already.) Usually the incident positron energy  $E_2$  and the angle  $\theta$  have certain width  $\Delta E_2$  and  $\Delta\theta$  and they cause the width  $W$  to the right of the peak in the spectrum. In the vicinity of the peak the shape of the spectrum is dominated by  $\Delta E_2$  and  $\Delta\theta$  and has very little to do with the radiative corrections. What one can calculate by using the standard method is the area under the curve between  $\omega_1^{\min}$  and  $c$  as a function of  $\Delta\omega_1$  as shown in Fig. 7 provided  $\Delta\omega_1$  is large compared with  $W$ . Even if in the ideal case where  $W$  is infinitely small  $\Delta\omega_1$  should not be taken too small<sup>11</sup> because of the infrared divergence difficulties inherent in the perturbation method. Since the area as a function of  $\Delta\omega_1$  can be calculated, we can obtain the spectrum itself in the region where  $\Delta\omega_1 \gg \omega$  by simply differentiating the expression for the area with respect to  $\Delta\omega_1$ .

Thus our experimental condition in the lab frame can be stated as "How many photons can be detected in a small angular range  $\Delta\theta$  with energy  $\omega_1 > \omega_1^{\min}$  if the incident positrons have energy  $E_2$ ?" In the center of mass system we have incident positron energy

$$\bar{E} = \sqrt{\frac{mE_2}{2}}, \quad \left( \bar{\gamma} \equiv \frac{\bar{E}}{m} = \sqrt{\frac{\gamma}{2}} \right), \quad (3-6)$$

the scattering angle  $\bar{\theta}$

$$1 - \cos\bar{\theta} \approx \frac{\gamma\theta^2}{1 + \frac{\gamma\theta^2}{2}}, \quad (3-7)$$

and the energy of the detected photon

$$\bar{\omega}_1 = \frac{k_1 (P_1 + P_2)}{\sqrt{(P_1 + P_2)^2}} \approx \frac{\omega_1 \left(1 + \frac{\gamma\theta^2}{2}\right)}{2\bar{\gamma}}. \quad (3-8)$$

From the above equations we can construct the phase space for the photon

$k_1$  in the center of mass system represented by an area ABCD in Fig. 8.

The horizontal line AB is obtained by setting  $\bar{\omega}_1 = \bar{E}_2$  where  $\bar{E}_2$  is given by Eq. (3-6).  $\theta_{\min}^{\max}$  is obtained from Eq. (3-7),

$$1 - \cos\theta_{\min}^{\max} = \frac{\gamma\theta_{\min}^{\max 2}}{1 + \frac{\gamma\theta_{\min}^{\max 2}}{2}}. \quad (3-9)$$

The line CD is obtained from Eqs. (3-8) and (3-7)

$$\bar{\omega}_1 = \omega_1^{\min} \frac{\left(1 + \frac{\gamma\theta^2}{2}\right)}{2\gamma} = \frac{\omega_1^{\min}}{2\gamma \cos^2 \frac{\bar{\theta}}{2}} \quad (3-10)$$

Now we know the infrared divergence occurs near the straight line AB and the main contribution to the cross section comes from the region of the phase space near the line AB. We are thus justified to replace the line CD by C'D' which is obtained by replacing  $\bar{\theta}$  by  $\bar{\theta}_{\text{ave}}$  in Eq. (3-10). For convenience we define

$$\Delta\bar{\theta} \equiv \bar{\theta}_{\text{max}} - \bar{\theta}_{\text{min}} = \frac{2\gamma\theta\Delta\theta}{\left(1 + \frac{\gamma\theta^2}{2}\right)^2 \sin\bar{\theta}} \quad (3-11)$$

and

$$\Delta\bar{\omega}_1 \equiv \bar{E} - \bar{\omega}_1^{\min} = \bar{E} \frac{\Delta\omega_1}{\omega_1^{el}(\theta_{\text{ave}})} \quad (3-12)$$

where  $\omega_1^{el}(\theta_{\text{ave}})$  is the peak energy of  $k_1$  in the laboratory system as shown in Fig. 7, and corresponds approximately to the value of  $\omega_1$  obtained from Eq. (2-8) with an average values of  $\theta$  and  $\gamma$ . Hereafter we assume  $\Delta\theta$  to be very small and simply write  $\omega_1^{el}$  for  $\omega_1^{el}(\theta_{\text{ave}})$ . Thus we have specified the phase space of  $k_1$  in the center of mass system.

We next determine the phase space of  $k_2$  and  $k_3$ . From energy and momentum conservation

$$\bar{\omega}_1 + \bar{\omega}_2 + \bar{\omega}_3 = 2\bar{E}, \quad (3-13)$$

and

$$\bar{k}_1 + \bar{k}_2 + \bar{k}_3 = 0, \quad (3-14)$$

we can show that for each value of  $\bar{k}_1$  the allowed values of  $\bar{k}_2$  and  $\bar{k}_3$  must be on the surface of an ellipsoid with  $\bar{k}_1$  vector connecting the two foci as shown in Fig. 9. The ellipsoid shrinks to a line when  $\bar{\omega}_1 = \bar{E}$  and has a maximum extension when  $\bar{\omega}_1 = \bar{\omega}_1^{\text{min}}$ . Thus the phase space of  $k_2$  and  $k_3$  can be represented by all the points inside the ellipsoid obtained by setting  $\bar{\omega}_1 = \bar{\omega}_1^{\text{min}}$ . In principle one has to treat  $k_2$  and  $k_3$  symmetrically since they are identical particles and both are undetected. However as is shown in the Appendix we need to consider only half of the phase space, Fig. 10, due to the symmetry between  $k_2$  and  $k_3$ . In this phase space only  $k_3$  but not  $k_2$  can become infrared. The distance from the point o to any point on the surface of this semiellipsoid gives the maximum value of  $\omega_3$ , and is a function of angle  $(\bar{\theta}_{13})$  between  $k_1$  and  $k_3$  in the center of mass system. Explicitly one obtains

$$\bar{\omega}_3^{\text{max}} = \frac{2\bar{E}\bar{\Delta\omega}_1}{\bar{E} + \bar{\Delta\omega}_1 + (\bar{E} - \bar{\Delta\omega}_1) \cos\bar{\theta}_{13}}, \quad (3-15a)$$

for

$$\cos\bar{\theta}_{13} > - \frac{\bar{E} - \bar{\Delta\omega}_1}{\bar{E} + \bar{\Delta\omega}_1} \equiv - \cos\beta = - \frac{1 - \frac{\Delta\omega}{\omega_1} \frac{1}{e\ell}}{1 + \frac{\Delta\omega}{\omega_1} \frac{1}{e\ell}};$$

and

$$\bar{\omega}_3^{\text{max}} = - \frac{\bar{E} - \bar{\Delta\omega}_1}{2\cos\bar{\theta}_{13}}, \quad (3-15b)$$



for

$$\cos\theta_{13} \leq - \frac{\bar{E} - \Delta\bar{\omega}_1}{\bar{E} + \Delta\bar{\omega}_1} .$$

Equation (3-15a) represents the equation for the ellipsoid and Equation (3-15b) represents the bottom flat surface in Fig. 10. Some simplification to the phase space of  $k_3$  can be obtained by explicitly considering the nature of the matrix elements.

There are 6 diagrams which contribute to the  $3\gamma$  annihilation process as shown in Fig. 6.  $k_3$  is not connected to the external charged lines in  $M_5$  and  $M_6$  and thus  $M_5$  and  $M_6$  are not infrared divergent as can be verified by explicit calculations. For simplicity of the calculation we shall ignore  $M_5$  and  $M_6$  and further the terms proportional to  $k_3$  in the numerator.<sup>12</sup> Then the cross section for  $3\gamma$  annihilation can be written as

$$\frac{d\sigma_{3\gamma}}{d\Omega} = - \frac{d\sigma_0}{d\Omega} \frac{\alpha}{4\pi^2} \int \frac{\bar{k}_3^2 d\bar{k}_3 d\bar{\Omega}_3}{\sqrt{\bar{k}_3^2 + \lambda^2}} \left( \frac{m^2}{(P_{23} k_3)^2} - \frac{2P_1 P_2}{(P_{13} k_3)(P_{23} k_3)} + \frac{m^2}{(P_{13} k_3)^2} \right) \quad (3-16)$$

In the center of mass system both  $P_1$  and  $P_2$  are extremely relativistic and the denominators in the integrand of Eq. (3-16) tell us that practically all  $k_3$  are emitted either along  $\bar{P}_1$  or  $\bar{P}_2$ . Thus we expect the result of the integration is quite insensitive to the detail shape of the phase space except in the vicinity of  $\bar{k}_3 \parallel \bar{P}_1$  and  $\bar{k}_3 \parallel \bar{P}_2$ . The maximum values of  $\bar{\omega}_3$  along  $P_1$  and  $P_2$  can be obtained from Eqs. (3-15a,b) by setting

$\bar{\theta}_{13} = \pi - \bar{\theta}$  and  $\bar{\theta}_{13} = \bar{\theta}$  respectively, and are to be denoted as  $\omega_3^{\max}(\bar{k}_3 // \bar{P}_1)$  and  $\omega_3^{\max}(\bar{k}_3 // \bar{P}_2)$  respectively. We have tacitly assumed that  $\bar{\omega}_3$  is much smaller compared with  $\bar{E}$  in order to obtain a very simple expression (Eq. 3-16) for the  $3\gamma$  annihilation cross section. But from Fig. 10 we see that even for small  $\Delta\bar{\omega}_1$ ,  $\bar{\omega}_3$  can be as large as  $\sim \frac{\bar{E}}{2}$ . However, as can be seen from Eq. (3-15) and Fig. 11, if

$$\pi - \beta \gg \bar{\theta} \gg \beta, \quad (3-17)$$

both  $\omega_3^{\max}(\bar{k}_3 // \bar{P}_1)$  and  $\omega_3^{\max}(\bar{k}_3 // \bar{P}_2)$  are always small compared with  $\bar{E}$  if  $\Delta\bar{\omega}_1$  is small. Hence we shall assume that inequalities (3-17) are satisfied.<sup>13</sup> The integration (3-16) is a familiar one occurring in every bremsstrahlung calculation. Past experiences<sup>14</sup> show that the phase space shown in Fig. 10 can be replaced by a sphere with a radius  $K_3^{\max}$  defined by a geometrical mean

$$\begin{aligned} K_3^{\max} &= \left[ \omega_3^{\max}(\bar{k}_3 // \bar{P}_1) \times \omega_3^{\max}(\bar{k}_3 // \bar{P}_2) \right]^{\frac{1}{2}} \\ &= 2\bar{E} \Delta\bar{\omega}_1 \left[ (\bar{E} + \Delta\bar{\omega}_1)^2 - (\bar{E} - \Delta\bar{\omega}_1)^2 \cos^2\theta \right]^{-\frac{1}{2}}. \end{aligned} \quad (3-18)$$

Carrying out the integration in this spherical phase space, and neglecting non-logarithmic terms, we obtain<sup>15</sup>

$$\frac{d\sigma_{3\gamma}}{d\Omega_{k_1}} = -\frac{d\sigma_0}{d\Omega} \frac{\alpha}{\pi} \left[ 2 \ln \frac{\bar{E}}{K_3^{\max}} \left( \ln \frac{4\bar{E}^2}{m^2} - 1 \right) + \frac{1}{2} K(P_1, P_2) + \frac{1}{2} K(P_1, P_2) - K(P_1, P_2) \right] \quad (3-19)$$

where  $K(P_i, P_j)$  is the infrared terms and defined by

$$K(P_i, P_j) = (P_i P_j) \int_0^1 \frac{\ln \frac{P^2 - x}{\lambda^2}}{P^2 x} dx \quad (3-20)$$

with  $P_x = P_i X + P_j(1-X)$ . It was emphasized by the author in previous works<sup>9,10</sup> that it is a good idea not to integrate terms like  $K(P_i, P_j)$  explicitly because they always cancel between elastic and inelastic radiative corrections. However, since we are going to use Harris and Brown's results on the elastic part we give the explicit expressions for  $K(P_i, P_j)$  in the center of mass system. (Of course the expression can be covariantized easily.)

$$K(P_1, P_1) = K(P_2, P_2) = \ln \frac{m}{\lambda} . \quad (3-21)$$

$$K(P_1, P_2) = \frac{\bar{E}^2 + \bar{P}^2}{2\bar{P} \bar{E}} \left[ \ln \frac{4\bar{P}^2}{\lambda^2} \ln \frac{\bar{E} + \bar{P}}{\bar{E} - \bar{P}} + \frac{1}{2} \ln^2 \frac{\bar{E} + \bar{P}}{2\bar{P}} - \frac{1}{2} \ln^2 \frac{\bar{E} - \bar{P}}{2\bar{P}} + \ln \frac{\bar{E}}{\bar{P}} \ln \frac{\bar{E} + \bar{P}}{\bar{E} - \bar{P}} - 2\Phi\left(\frac{\bar{E} + \bar{P}}{2\bar{E}}\right) + 2\Phi\left(\frac{\bar{E} - \bar{P}}{2\bar{E}}\right) \right] . \quad (3-22)$$

$$\approx \frac{\bar{E}^2 + \bar{P}^2}{2\bar{P} \bar{E}} \left[ \ln \frac{4\bar{P}^2}{\lambda^2} \ln \frac{\bar{E} + \bar{P}}{\bar{E} - \bar{P}} - \frac{1}{2} \ln^2 \frac{4\bar{P}^2}{m^2} - \frac{\pi^2}{6} \right] \quad (3-23)$$

Experimentally meaningful cross section can be obtained by adding Eq. (3-19)

to Eq. (3-4) and we obtain finally

$$\frac{d\sigma}{d\Omega} = \frac{d\sigma_{2\gamma}}{d\Omega} + \frac{d\sigma_{3\gamma}}{d\Omega} = \frac{d\sigma_0}{d\Omega} (1 + \delta), \quad (3-24)$$

with

$$\delta = \frac{-2\alpha}{\pi} \left\{ \ln \frac{\bar{E}}{K_3^{\max}} - \frac{3}{4} \right\} \left( \ln \frac{4\bar{E}^2}{m^2} - 1 \right) + \frac{f}{2}, \quad (3-25)$$

where  $f$  is the function defined in Eq. (3-5), and is numerically very small in the range where inequalities (3-17) hold.<sup>16</sup>

The radiative correction  $\delta$  in Eq. (3-24) can be written explicitly in terms of laboratory quantities by the following substitutions:

$$\frac{4\bar{E}^2}{m^2} = \frac{2E}{m} = 2\gamma, \quad (3-26)$$

$$\frac{\bar{E}}{K_3^{\max}} \approx \frac{\omega_1 e l}{\Delta\omega_1} \frac{\sqrt{\gamma\theta^2}}{\left(1 + \frac{\gamma\theta^2}{2}\right) \sqrt{2}}, \quad (3-27)$$

$$\kappa = \frac{2\omega_1 e l}{m} \approx \frac{2\gamma}{1 + \frac{\gamma\theta^2}{2}}, \quad (3-28)$$

and

$$\tau = \frac{2\omega_1 e l}{m} \approx \frac{\gamma^2\theta^2}{1 + \frac{\gamma\theta^2}{2}}. \quad (3-29)$$

In summary, Eq. (3-24) gives the area under the curve of Fig. 7 from  $\omega_1^{\min}$  to  $c$  as a function of  $\Delta\omega_1$  in the range

$$\omega_1^{el} 0.1 > \Delta\omega_1 > W, \quad (3-30)$$

provided the angle  $\theta$  is such that

$$\frac{\omega_1}{\Delta\omega_1} \gg \frac{\gamma\theta^2}{2} \gg \frac{\Delta\omega_1}{\omega_1}. \quad (3-31)$$

The lower limit of  $\Delta\omega_1$  in (3-30) is necessary because near the peak in Fig. 7, the shape of the spectra is mainly determined by  $\Delta E_2$  and  $\Delta\theta$  and further even if  $\Delta E_2$  and  $\Delta\theta$  were zero (i.e.  $\omega=0$ ),  $\Delta\omega_1$  should not be taken too small because of infrared divergence difficulties, i.e. Eq. (3-24) diverges as  $\Delta\omega_1 \rightarrow 0$ . A proper criteria to ascertain that we are not in the infrared region is that  $\Delta\omega_1$  should be taken large enough such that<sup>17</sup>  $-\delta \lesssim 0.2$ . On the other hand the upper limit of  $\Delta\omega_1$  and inequalities (3-31) were imposed because we had assumed  $\bar{\omega}_3$  to be small compared with  $\bar{E}$  in order to obtain Eq. (3-16). Inequalities (3-31) are merely the reexpression of the C.M. condition (3-17) in terms of lab quantities.

Differentiating Eq. (3-24) with respect to  $\Delta\omega_1$  we obtain the spectral distribution of  $\omega_1$  at angle  $\theta$  in the lab system,

$$\frac{d^2\sigma_{3\gamma}}{d\Omega_{k_1} d\omega_1} = \frac{\partial}{\partial \Delta\omega_1} \left( \frac{d\sigma}{d\Omega_{k_1}} \right) = \frac{d\sigma_0}{d\Omega} \frac{2\alpha}{\pi} \left( \ln \frac{2E_2}{m} - 1 \right) \frac{1}{\omega_1^{el} - \omega_1}, \quad (3-32)$$

which is correct only if  $\Delta\omega_1 = \omega_1^{el} - \omega_1$  and  $\theta$  are such that (3-30) and (3-31) are satisfied.

#### 4. NUMERICAL EXAMPLES

In order to facilitate numerical computations we shall rewrite all our formulae in more compact forms. We are mainly interested in the regions of  $\theta$  and  $\Delta\omega_1$  specified by inequalities (2-11), (3-30) and (3-31). Let us introduce two new symbols

$$z = \frac{\gamma\theta^2}{2} \quad (4-1)$$

$$R = \frac{\omega_0 \ell}{\Delta\omega_1} \quad (4-2)$$

The lowest order cross section for  $e^+ + e^- \rightarrow 2\gamma$  can be written as (see Eq. 2-13)

$$\frac{d\sigma_0}{d\Omega_k} \approx \frac{r_0^2}{2} \frac{1}{(1+z)^2} \left( \frac{1}{z} + z \right). \quad (4-3)$$

The radiative corrections  $\delta$  can be written as (see Eq. 3-25)

$$\delta = -\frac{2\alpha}{\pi} \left\{ \ln \left( R \frac{\sqrt{z}}{1+z} \right) - \frac{3}{4} \right\} (\ln 2\gamma - 1) + Y, \quad (4-4)$$

where

$$\begin{aligned} Y = & \frac{\alpha}{\pi} \frac{1}{\left(z + \frac{1}{z}\right)} \left\{ \left(1+z + \frac{1}{2z}\right) \right\} \left\{ \ln^2 \left(1 + \frac{1}{z}\right) - \ln \left(1 + \frac{1}{z}\right) \right\} \\ & + \left(1 + \frac{1}{z} + \frac{z}{2}\right) \left\{ \ln^2 (1+z) - \ln (1+z) \right\} \\ & + \left(\frac{1}{z} - z\right) \ln z + \pi^2 \left\{ \frac{1}{3} + \frac{1}{12} \left(z + \frac{1}{z}\right) \right\}. \end{aligned} \quad (4-5)$$

The spectra of the photon for  $e^+ + e^- \rightarrow 3\gamma$  can be written as (see Eq. 3-32)

$$\frac{d^2\sigma_{3\gamma}}{d\Omega_{k_1} d\omega_1} = \frac{\alpha r_0^2}{\pi} \frac{1}{(1+z)} \left(z + \frac{1}{z}\right) (\ln 2\gamma - 1) \frac{R}{E_2} \quad (4-6)$$

The quantity  $Y(z)$  has a rather complicated expression but numerically it is very small. For example

$$Y(10) = Y(0.1) = 0.0024$$

$$Y(1) = 0.004$$

The numerical values for  $\delta$  are given for  $\gamma = 3 \times 10^4$  (i.e.  $E_2 = 15$  BeV) and  $z = 1$ ,

$$R = 100 \quad \delta = -0.207$$

$$R = 50 \quad \delta = -0.175$$

$$R = 25 \quad \delta = -0.142$$

$$R = 10 \quad \delta = -0.10$$

$$R = 5 \quad \delta = -0.068$$

## 5. CONCLUDING REMARKS

A. The purpose of writing this paper is three-fold.

1. To obtain useful formulae concerning the use of  $\gamma$  rays from  $e^+e^- \rightarrow 2\gamma$  as a source for high energy  $\gamma$  rays. It is hoped that various formulae and considerations given here may be of some help to the experimentalists in designing the experiments.

2. To show how this type of calculation can be done in order to take into account the realistic experimental requirements.

3. As a byproduct of this calculation, we observe that there is no term such as  $\frac{\alpha}{\pi} \ln^2 \frac{4\bar{E}^2}{m^2}$  in our expression for  $\delta$  (see Eq. (3-31)). Such a term occurs only in the infrared term  $K(P_1, P_2)$  which is cancelled completely after addition of elastic and inelastic cross sections as previously observed.<sup>10</sup> Thus we conclude that the appearance of such a term in Brown and Feynman and Harris and Brown's results is purely due to those authors choice of phase space for  $k_3$ , namely  $\omega_3$  is isotropic and  $\ll m$  in the lab frame. As emphasized previously that this kind of term is very undesirable. If, irrespective of how one chooses the phase space for  $k_3$ , terms such as  $\frac{\alpha}{\pi} \ln^2 \frac{4\bar{E}^2}{m^2}$  occur in  $\delta$ , it means that quite independent of infrared catastrophies the perturbation expansion is not valid at energies higher than the value at which  $\frac{\alpha}{\pi} \ln^2 \frac{4\bar{E}^2}{m^2} \sim 1$ . (This will occur at around  $\bar{E} \sim \text{BeV.}$ ) In other words, the existence of such terms in B.F. and H.B. and disappearance of such terms in our expression simply indicate that such terms are closely related to the infrared catastrophe of the perturbation expansion and can be gotten rid of if one chooses the phase for  $\omega_3$  to be such that  $\omega_3^{\text{max}} \gg m$  in the center of mass system.

B. It is interesting to notice the similarity between our expression for  $\delta$  (see Eq. 3-25) and the Schwinger's radiative corrections to the potential scattering,

$$\delta_{\text{Schwinger}} \approx \frac{-2\alpha}{\pi} \left\{ \left( \ln \frac{E}{\Delta E} - \frac{13}{12} \right) \left( \ln \frac{-q^2}{m^2} - 1 \right) + \frac{17}{36} \right\}. \quad (5-1)$$



The similarity can be made more striking if we decompose  $\delta_{\text{Schwinger}}$  into the contributions from the vacuum polarization, the vertex part and the bremsstrahlung:

$$\delta_{\text{Schwinger}} = \delta_{\text{vac}} + \delta_{\text{vertex}} + \delta_{\text{brem}}, \quad (5-2)$$

where

$$\delta_{\text{vac}} = \frac{2\alpha}{\pi} \left[ \frac{-5}{9} + \frac{1}{3} \ln \left( \frac{-q^2}{m^2} \right) \right], \quad (5-3)$$

$$\delta_{\text{vertex}} = \frac{-2\alpha}{\pi} \left[ \frac{1}{2} K(P_1, P_3) - \frac{1}{2} K(P_1, P_1) - \frac{3}{4} \ln \left( \frac{-q^2}{m^2} \right) + 1 \right], \quad (5-4)$$

$$\delta_{\text{brem}} = \frac{-2\alpha}{\pi} \left[ \frac{-1}{2} K(P_1, P_3) + \frac{1}{2} K(P_1, P_1) + \ln \frac{E}{\Delta E} \left( \ln \frac{-q^2}{m^2} - 1 \right) \right]. \quad (5-5)$$

Now if we omit  $\delta_{\text{vac}}$  and consider

$$\delta_{\text{vertex}} + \delta_{\text{brem}} = \frac{-2\alpha}{\pi} \left[ \left( \ln \frac{E}{\Delta E} - \frac{3}{4} \right) \left( \ln \frac{-q^2}{m^2} - 1 \right) + \frac{1}{4} \right], \quad (5-6)$$

we arrived at a formula almost identical to Eq. (3-25) if we make the following substitutions:

$$\frac{E}{\Delta E} \rightarrow \frac{\bar{E}}{K_3^{\text{max}}} \quad (5-7a)$$

$$-q^2 \rightarrow 4\bar{E}^2 \quad (\text{in the more usual notations } -t \rightarrow s). \quad (5-7b)$$

It is obvious why one should omit  $\delta_{\text{vac}}$ , because there is no vacuum polarization in our problem. It is also quite obvious why by making substitutions (5-7 a,b) on Eq. (5-5) we can obtain our Eq. (3-19). However it is

not quite obvious that by making a substitution  $-t \rightarrow s$  into the ordinary vertex correction one obtains the bulk of the virtual radiative corrections represented by Eq. (3-4).<sup>18</sup>

C. The present calculation can be easily adapted to the need of the colliding beam experiment proposed at Stanford. The purpose of investigating the reaction such as  $e^+ + e^- \rightarrow 2\gamma$  in the colliding experiment is to test the validity of quantum electrodynamics at high energies. Due to the background bremsstrahlungs, the experiment will probably be done by detecting two photons in coincidence and each photon detector having fairly good energy and angular resolutions. The lowest order cross section can be obtained from Eq. (2-4) by covariantizing the expression inside the bracket and recalculating the function A which represents the phase space and flux density. The result is

$$\begin{aligned} \frac{d\sigma_o}{d\Omega_{K_1}} &= \frac{r_o^2 m^2}{8\bar{P}\bar{E}} \left\{ \frac{\bar{E} + \bar{P} \cos\bar{\theta}}{\bar{E} - \bar{P} \cos\bar{\theta}} + \frac{\bar{E} - \bar{P} \cos\bar{\theta}}{\bar{E} + \bar{P} \cos\bar{\theta}} + 4m^2 \left( \frac{1}{\bar{E}^2 - \bar{P}^2 \cos^2\bar{\theta}} - \frac{m^2}{(\bar{E}^2 - \bar{P}^2 \cos\bar{\theta})^2} \right) \right\} \\ &\approx \frac{r_o^2 m^2}{8\bar{E}^2} \left\{ \cot^2 \frac{\bar{\theta}}{2} + \tan^2 \frac{\bar{\theta}}{2} \right\} \end{aligned} \quad (5-8)$$

The second equation holds only if  $\bar{\theta}$  and  $\bar{E}_2$  satisfies

$$\sin\bar{\theta} \gg \frac{1}{\gamma} \ll 1. \quad (5-9)$$

The radiative correction can be calculated by using Eq. (3-25). The only thing one has to do is to relate  $K_3^{\max}$  to the energy and angular resolutions of the detecting system. If  $\Delta\theta$  is negligible and further if  $\Delta\bar{\omega}_1$  is the smaller one of energy resolutions of the two detectors, then Eq. (3-18) can be used as  $K_3^{\max}$ .

## 6. ACKNOWLEDGEMENTS

The author wishes to thank Professor L. M. Brown for classifications on several points in the papers by Brown and Feynman and Harris and Brown. He also wishes to thank Dr. Z.G.T. Guiragossian for conversations concerning experimental matters.

## APPENDIX I

In applying the Feynman rules to calculate the transition probabilities involving identical particles in the final states considerable care must be exercised. Take the example of reaction  $e^+ + e^- \rightarrow k_1 + k_2 + k_3$  in the C.M. system. Because of energy-momentum conservation only momenta of two particles (say  $\vec{k}_1$  and  $\vec{k}_2$ ) are needed to determine the kinematics completely. Suppose we have two detectors A and B. We may arbitrarily assign the photon detected by A to be  $k_1$  and that detected by B to be  $k_2$ , and calculate the cross section according to the standard rule,

$$d\sigma = (2\pi)^4 \frac{1}{4 \left( (P_1 P_1)^2 - m_1^2 m_2^2 \right)^{\frac{1}{2}}} \frac{1}{(2\pi)^{3 \times 3}} \int \frac{d^3 k_1}{2\omega_1} \frac{d^3 k_2}{2\omega_2} \frac{d^3 k_3}{2\omega_3} \delta^4(p_f - p_i) S \left| \sum_{i=1}^6 M_i \right|^2 \quad (\text{A-1})$$

where  $S$  is average over initial spin and sum over the final polarizations and  $M_i$ 's are the matrix element written according to the standard rule. (We normalize one particle per  $(2E)^{-1} \text{cm}^3$  for each particle.) The integral is to be taken in the range specified by detectors A and B. Now suppose the detector B is removed, do we get the right result by just integrating over all  $d^3 k_2$ ? The answer is no. The expression (A1) must be divided by 2 and then integrate over all possible  $d^3 k_2$ . To show this, consider an event where one of three photons goes into A and another into B. The probability of this event (see Fig. 11a) is independent of whether there is a detector at B or not. Now corresponding to this event, there are two possibilities, either  $k_2$  goes into B or  $k_3$  goes into B as shown in Fig. 11b and 11c. Both of these possibilities occur when there is no detector at B. But now as soon

as we put a detector in B, the situation represented by Fig. 11c is excluded because we said the photon detected by B is called  $k_2$ . This proves our assertion. The result can be generalized to  $n$  identical particles in the final states. We need  $n-1$  detectors to determine the kinematics of the problem. Thus if there are  $n-1$  detectors we use the standard rule. If we have  $n-2$  detectors we divide the whole expression by 2. If there are  $n-d$  detectors we divide the standard expression by  $d!$ . Specifically if there is no detector (i.e. total cross section) we have to divide the Eq. (A-1) by  $n!$

The arguments given above can be used in our calculation of spectra of  $k_1$  due to  $e^+ + e^- \rightarrow 3\gamma$ . The radiative corrections calculated by Brown and Feynman and Harris and Brown apply only to the coincidence experiments. Since we are not measuring  $k_2$  and  $k_3$  we have to integrate over all the phase space of  $k_2$  and  $k_3$  and divide it by  $2!$  according to our prescription. The phase space of  $k_2$  and  $k_3$  can be represented as an ellipsoid as shown in Fig. 9. Now the matrix element  $|M|^2$  is symmetric with respect to interchange of  $k_2 \leftrightarrow k_3$ . Thus instead of integrating  $k_2$  and  $k_3$  in the whole phase space and divide it by  $2!$ , we may equivalently integrate half of the phase space as shown in Fig. 10. Now in this modified phase space  $k_2$  is never small and thus infrared divergence occurs only when  $k_3 \rightarrow 0$ , although both  $k_2$  and  $k_3$  can become infrared in the complete phase space.

## REFERENCES AND FOOTNOTES

1. J. Ballam and Z.G.T. Guiragossian, "Almost monochromatic photon beams at the Stanford Linear Accelerator Center." Proceedings of the International Conference on High-Energy Physics, Dubna, 1964.
2. Swanson, Iddings and Tsai, to be published.
3.  $\sigma_x$ ,  $\sigma_y$  and  $\sigma_z$  are usual  $2 \times 2$  Pauli matrices.
4. There is an error in Eq. (12-48) of Jauch and Rohlich: "Theory of photons and electrons." First Edition. In the Second Edition the correct formula was given.
5. I. Harris and L. M. Brown, Phys. Rev. 105, 1656 (1957). Hereafter referred to as H. B.
6. L. M. Brown and R. P. Feynman, Phys. Rev. 85, 231 (1951). Hereafter referred to as B. F.
7. We give this expression in detail because there are two misprints in Eq. 8, and wrong sign for Eq. (8a) of H. B. The present author did not check their calculation in complete detail. The errors were found by comparing with the results of B. F. According to Professor Brown, the results in B. F. are more correct.
8. This expression is very similar to Eq. 43 of B. F. except for the terms proportional to  $\pi^2$  in  $f$ .
9. Y. S. Tsai, Phys. Rev. 122, 1898 (1961).
10. The advantage of using the center of mass system is that it is easier to see under what conditions the  $k_3$  in the numerator of the matrix element can be neglected and obtain an extremely simple expression such as Eq. (3-16). From our considerations it can be concluded that in order to neglect  $k_3$  in the

numerator, it is not necessary to assume  $\omega_3$  to be much smaller than  $m$  in the laboratory system as was done in B. F. and H. B. As will be argued in Section 5, in the regions where  $\omega_3 \ll m$  in the lab system, the perturbation expansion is not valid due to the existence of terms like  $\frac{\alpha}{\pi} \ln^2 2\gamma$  in the radiative corrections  $\delta$ . Similar consideration was done by the author for the radiative correction to the  $e$ - $e$  scattering in the laboratory system. See Section 5 of the paper Y. S. Tsai, Phys. Rev 120, 269 (1960).

11. See footnote 17.
12. The approximations made here are certainly the most serious ones and impose severe limitations to the range of applicability of our result, represented by the first inequality in (3-30) and inequalities (3-31). The problem that one has to investigate is whether the curve in Fig. 7 goes down monotonically to the low energy end or will it go up again and give some additional (unwelcome) low energy photons. The author tends to believe the latter because a positron can first emit a high energy photon and then annihilate at a very low energy at which the cross section is very large. (A similar phenomenon is well known in the bremsstrahlung produced by coulomb scatterings.) Fortunately the exact calculation of low energy end of the spectrum can be done without much difficulty with the help of a computer. A computer can take traces, sum the tensor indices, do necessary cancellations, sorting out terms in a convenient order and obtain an analytical expression in less than one hour for a job which takes about six months for a physicist to do by paper and pencil. Two working computer procedures are available at Stanford, one by

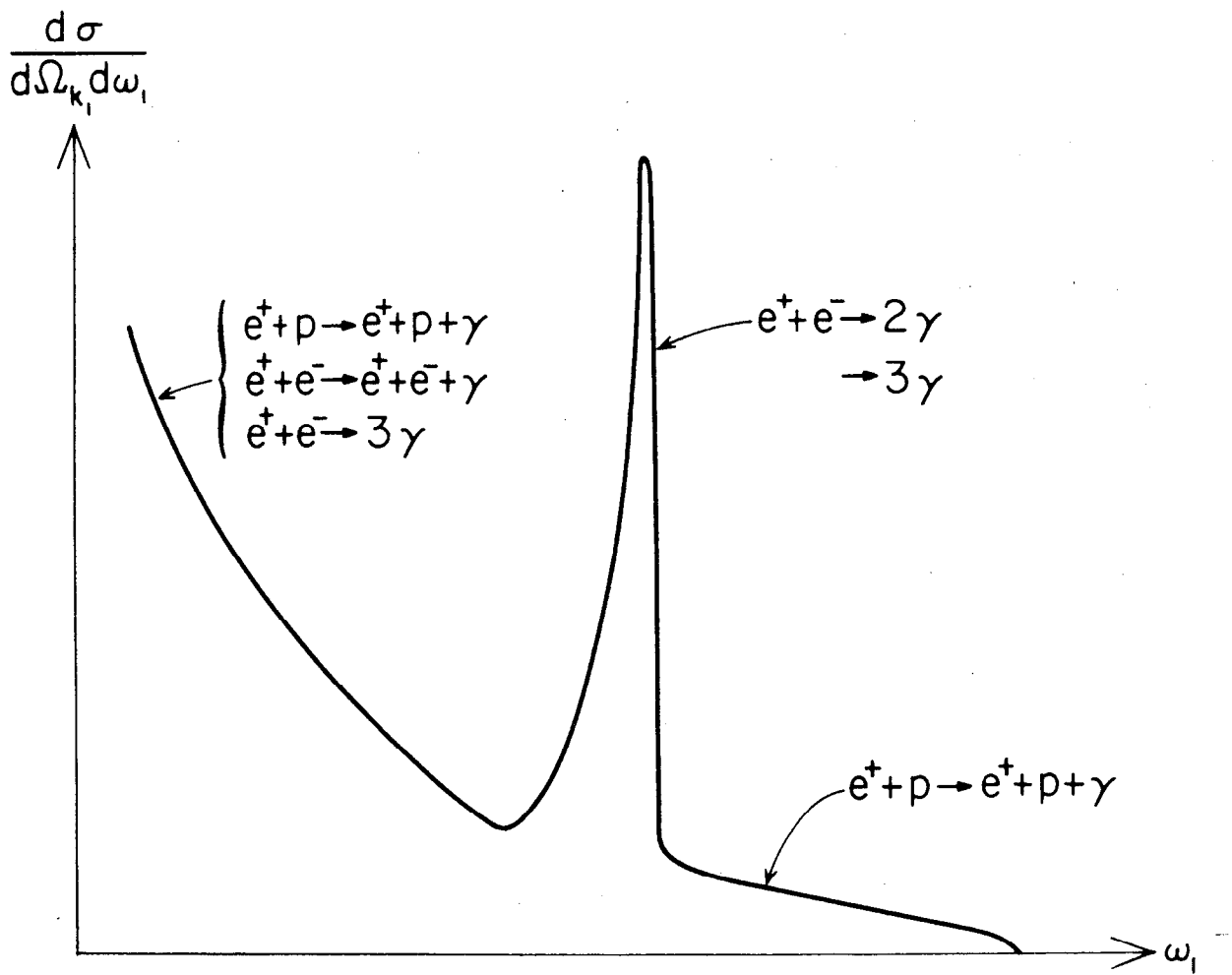
S. Swanson and another by A. Hearn, both of the Physics Department, Stanford University.

13. Inequalities (3-17) reduce to (3-31) in the laboratory system. Fortunately the angular range most convenient for the experimentalists<sup>1</sup> is in the vicinity of  $\gamma\theta^2/2 \sim \frac{1}{4}$  to 4 and thus these inequalities are easily satisfied.
14. See the discussion concerning Eq. (1-4) of Ref. 9.
15. See D. R. Yennie, S. C. Frantschi, H. Suura: *Annals of Physics* 13, 379 (1961), Appendix C.
16. See Section 4 for numerical examples, ( $-\alpha/\pi f = Y$ ).
17. If we believe in Schwinger's conjecture that the radiative corrections to all order can probably be written as  $e^\delta = 1 + \delta + \frac{\delta^2}{2!} + \dots$ , then for  $-\delta \leq 0.2$ , the next order correction will be expected to be less than 2%.
18. Brown and Feynman's results (Ref. 6) show that after renormalization and infrared cancellation, only the matrix element represented by J in Fig. 5 contains logarithmic terms when inequalities (3-3a,b) are satisfied. Thus our observation can be stated simply that the bulk of the contribution from the matrix element J to the radiative corrections can be obtained from the Schwinger vertex correction by a substitution  $-t \rightarrow s$ .



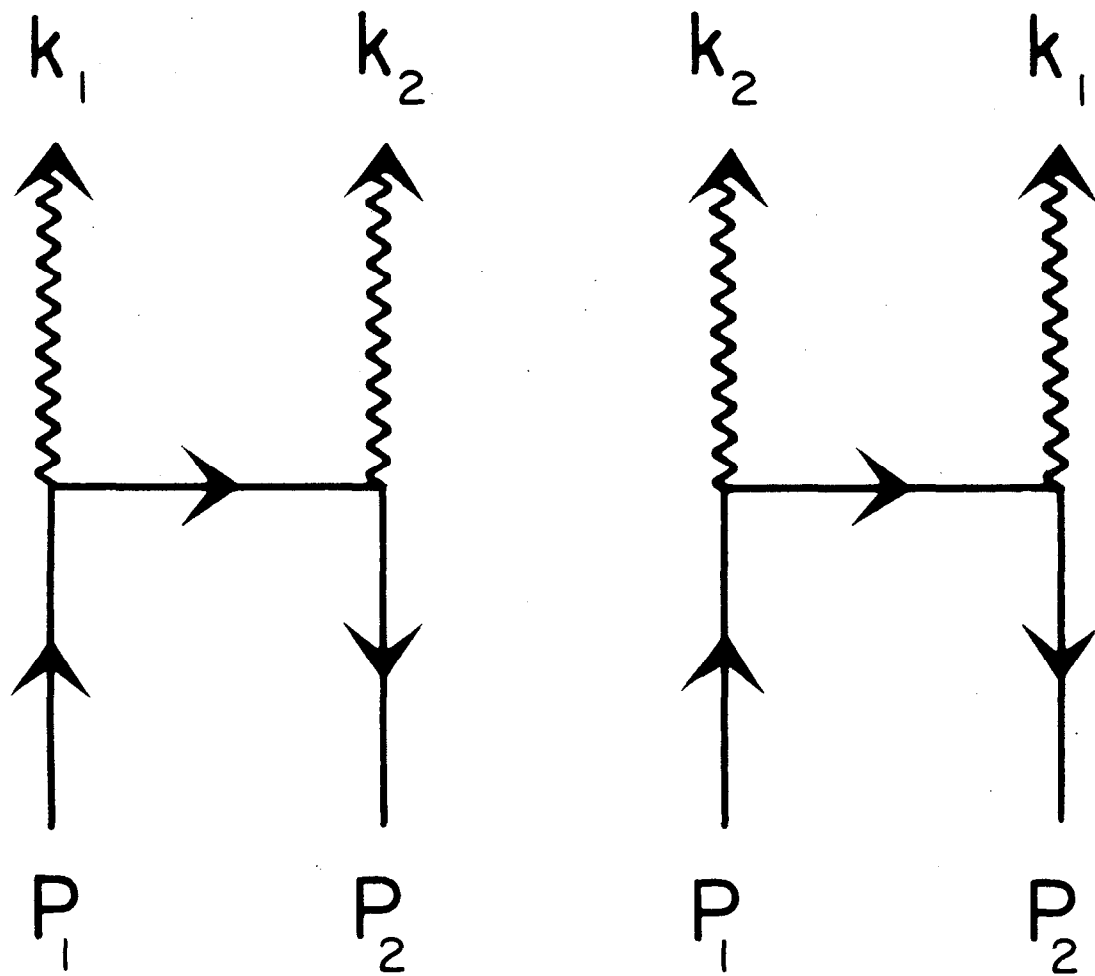
## LIST OF FIGURES

1. A typical gamma spectrum of positron hydrogen atom collision at a fixed angle.
2. Lowest order Feynman diagrams for the interaction  $e^+ + e^- \rightarrow 2\gamma$ .
3. Coordinate system used in the discussion of polarization of photons.  $k_2$  is chosen to be on the x-z plane.
4. Polarization vectors used in the definition of Stokes parameters for the photon  $k_1$ .
5. Feynman diagrams for virtual radiative corrections.
6. Feynman diagrams for real radiative corrections.
7. A typical energy spectrum of the photon at a fixed angle. The point  $\omega_1^{el}(\theta_{ave})$  is chosen to be the value of  $\omega_1$  determined by two body final state kinematics at the average angle of the detector.  $\Delta\omega_1$  should be chosen such that  $\bar{\omega} \ll \Delta\omega_1 \ll \omega_1^{el} 0.1$ .
8. The phase space for  $k_1$  in the center of mass system is represented by the area ABCD. We approximate ABCD by ABC'D'.
9. An ellipsoid representing the phase space for  $k_2$  and  $k_3$  in the center of mass system.  $\bar{k}_1$  connects the two foci of the ellipsoid. The ellipsoid has a maximum extension when  $\bar{\omega}_1 = \bar{\omega}_1^{min}$ .
10. The semiellipsoid to be used to determine  $\bar{\omega}_3^{max}$  as a function of  $\theta_{13}$  (angle between  $\bar{k}_1$  and  $\bar{k}_3$ ).
11. Three identical particles in the final state. (a) One particle  $k_1$  goes into detector A and another goes into direction B. (b)  $k_2$  goes into B. (c)  $k_3$  goes into B.



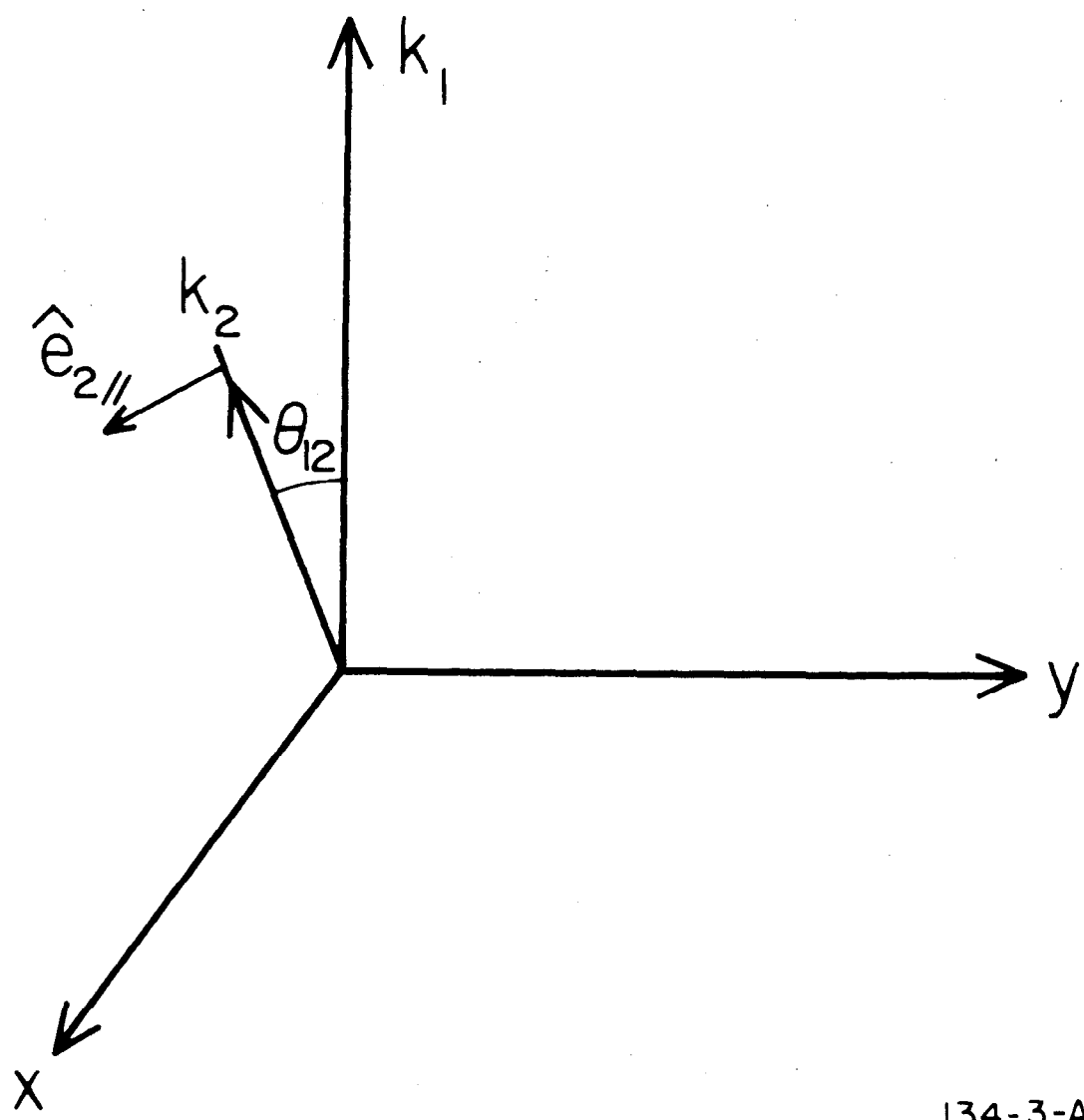
134-1-A

FIGURE 1



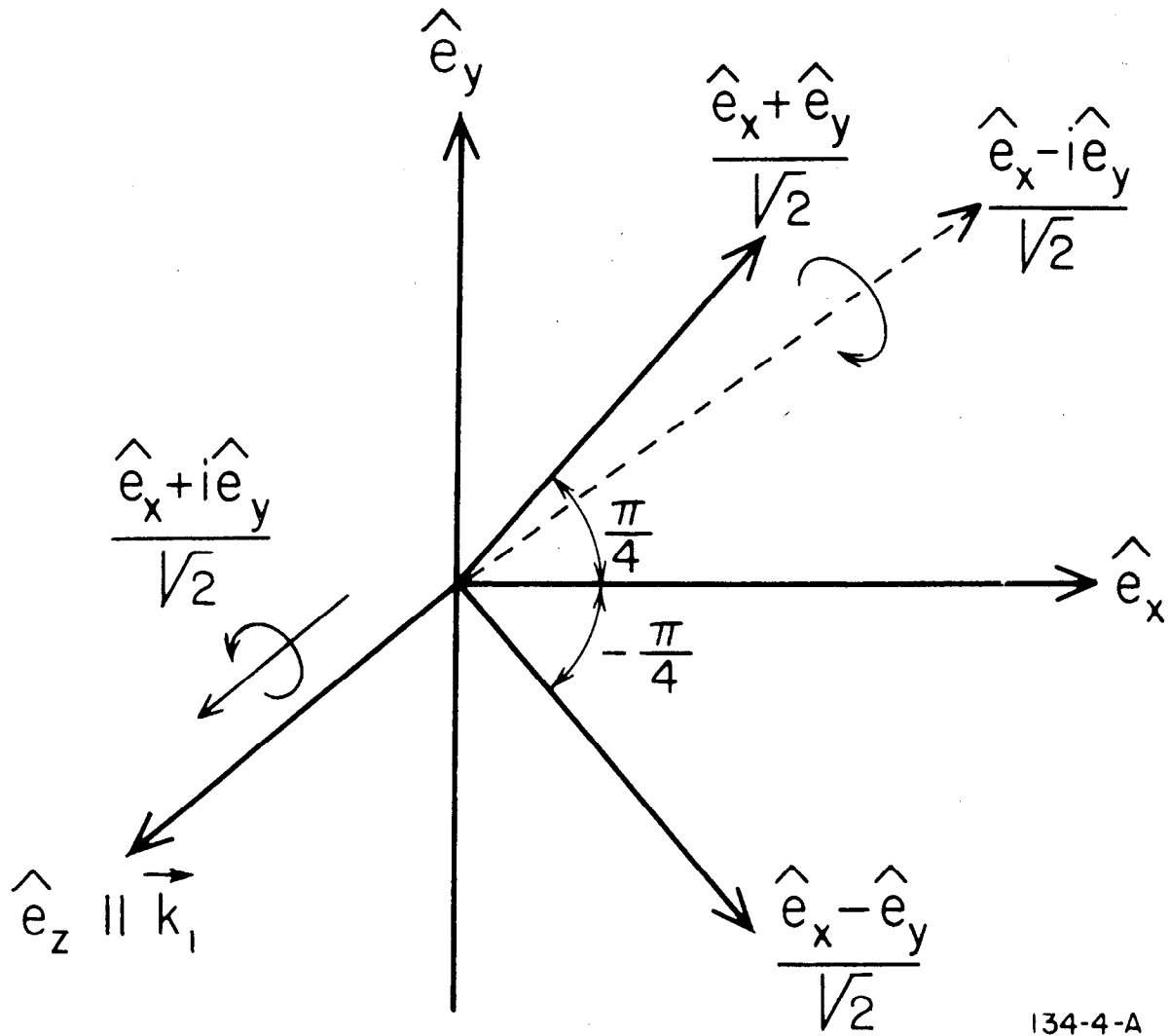
134-2-A

FIGURE 2



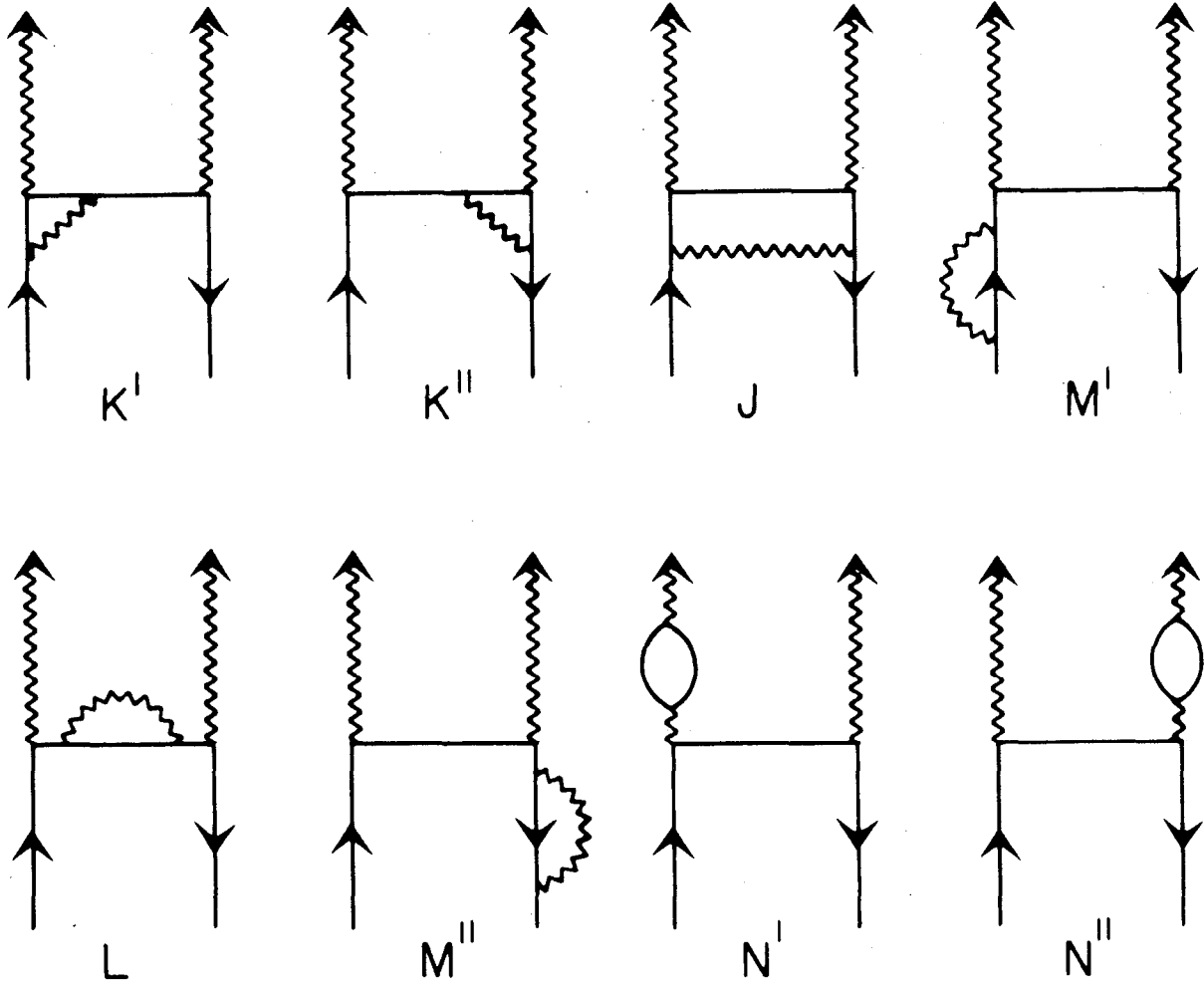
134-3-A

FIGURE 3



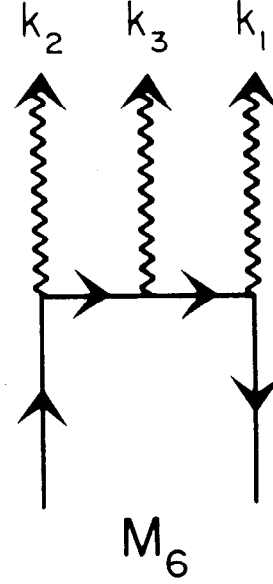
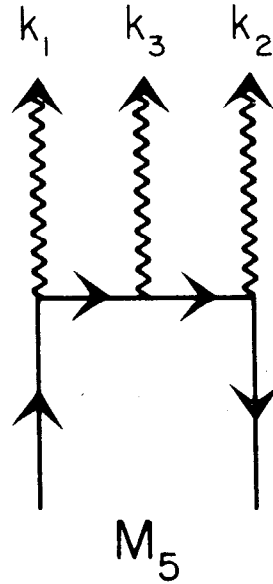
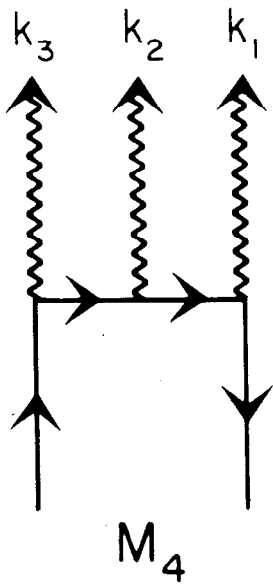
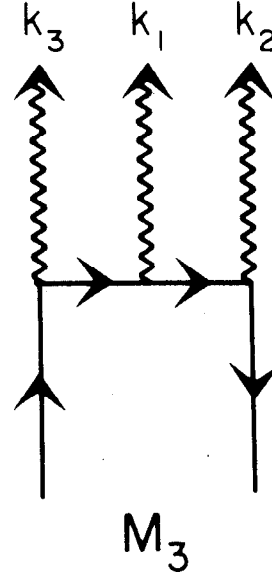
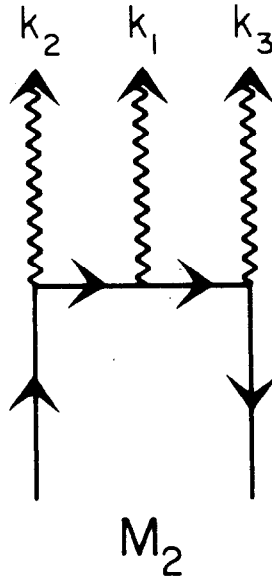
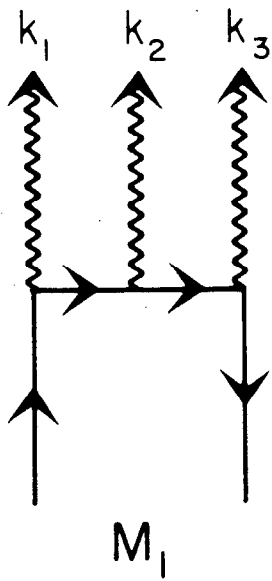
134-4-A

FIGURE 4



134-5-A

FIGURE 5



134-6-A

FIGURE 6

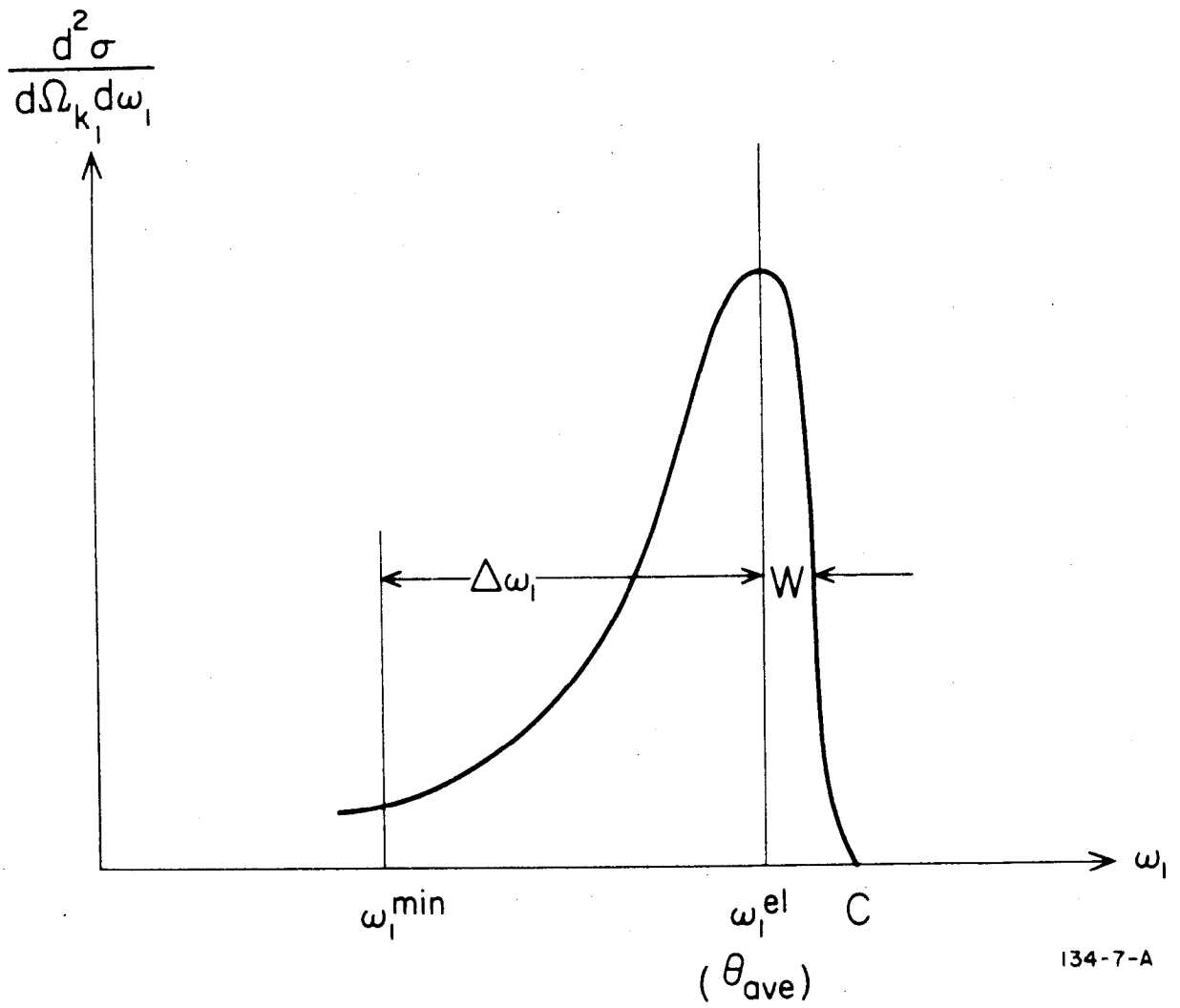


FIGURE 7



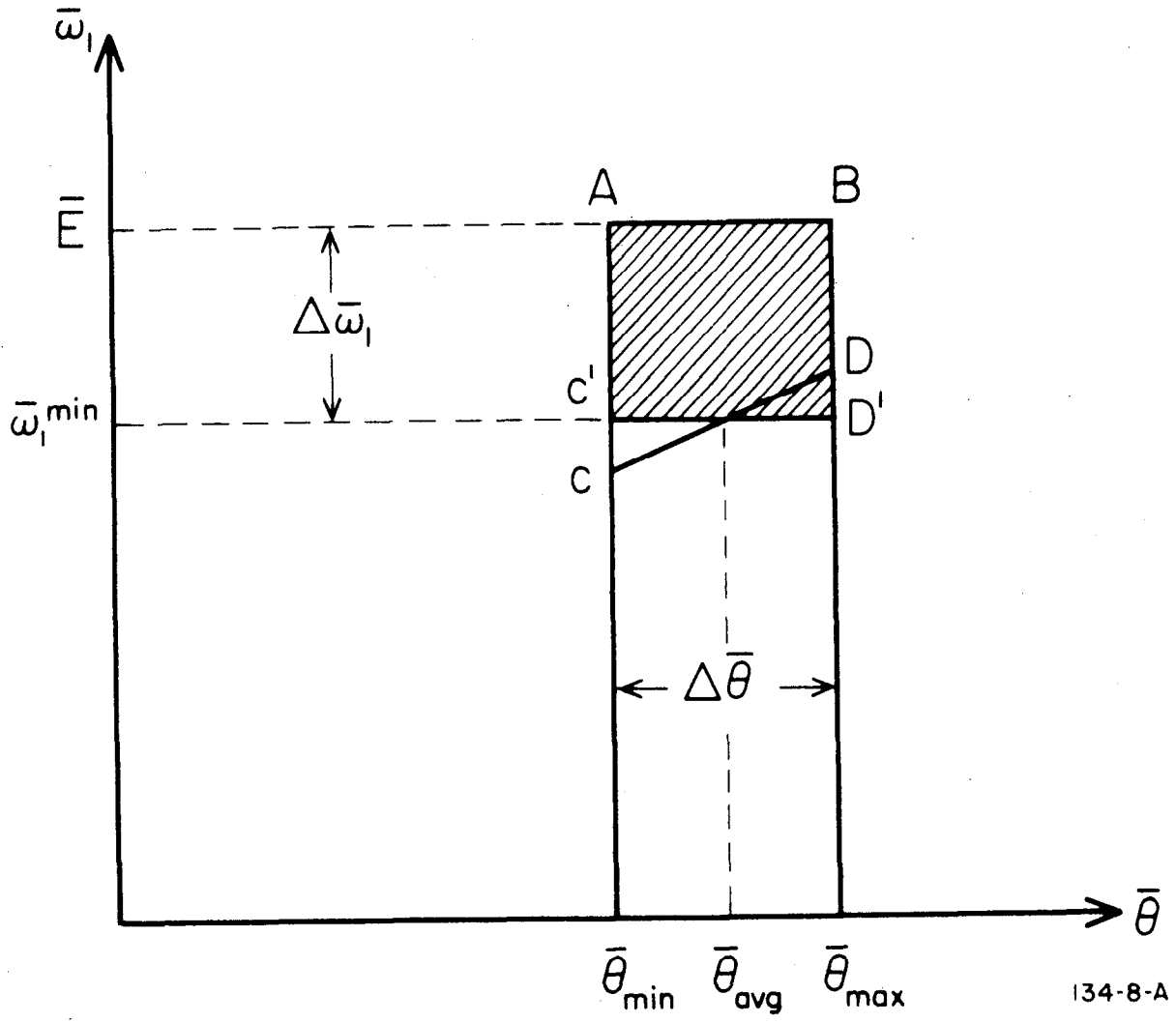
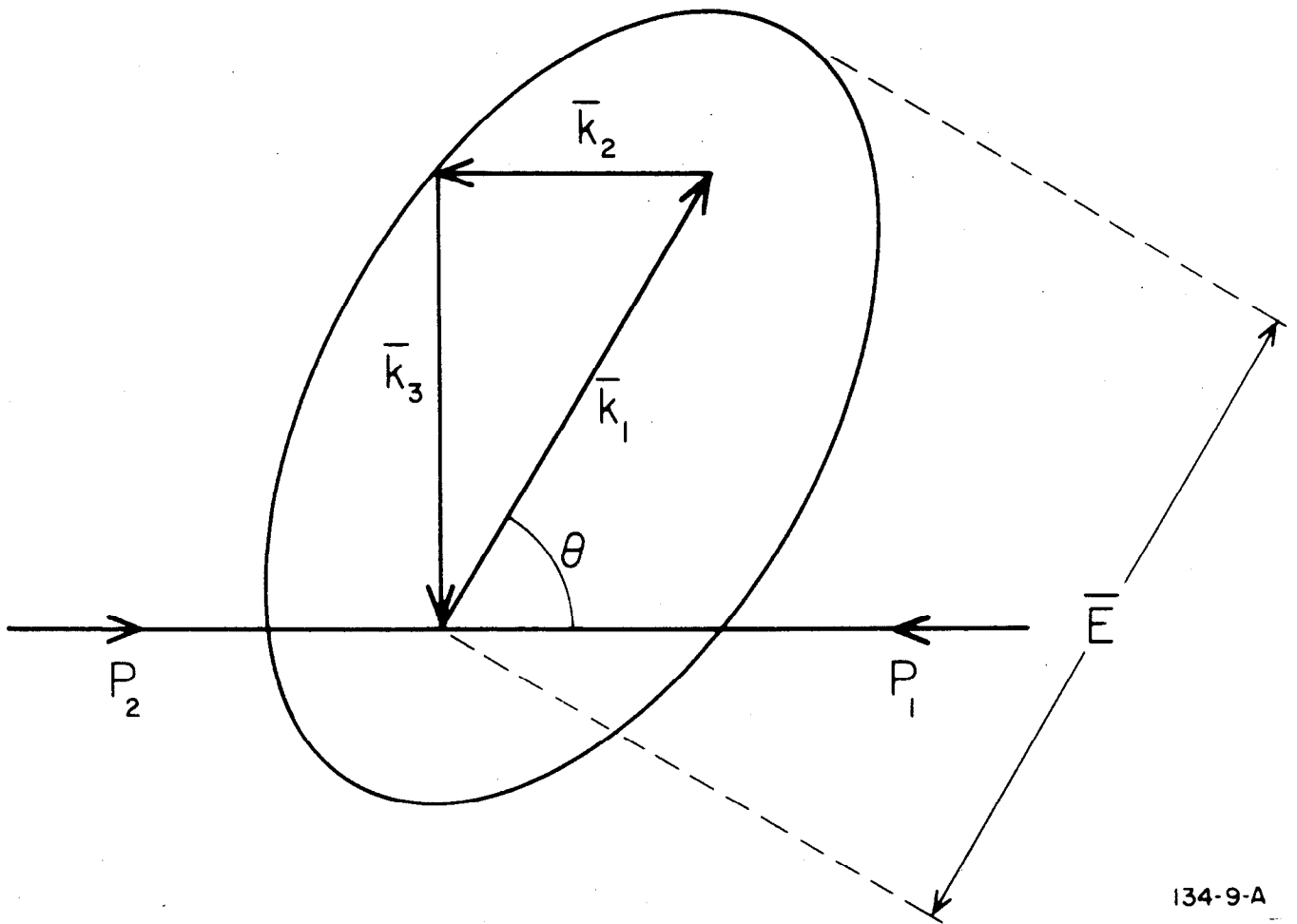


FIGURE 8



134-9-A

FIGURE 9

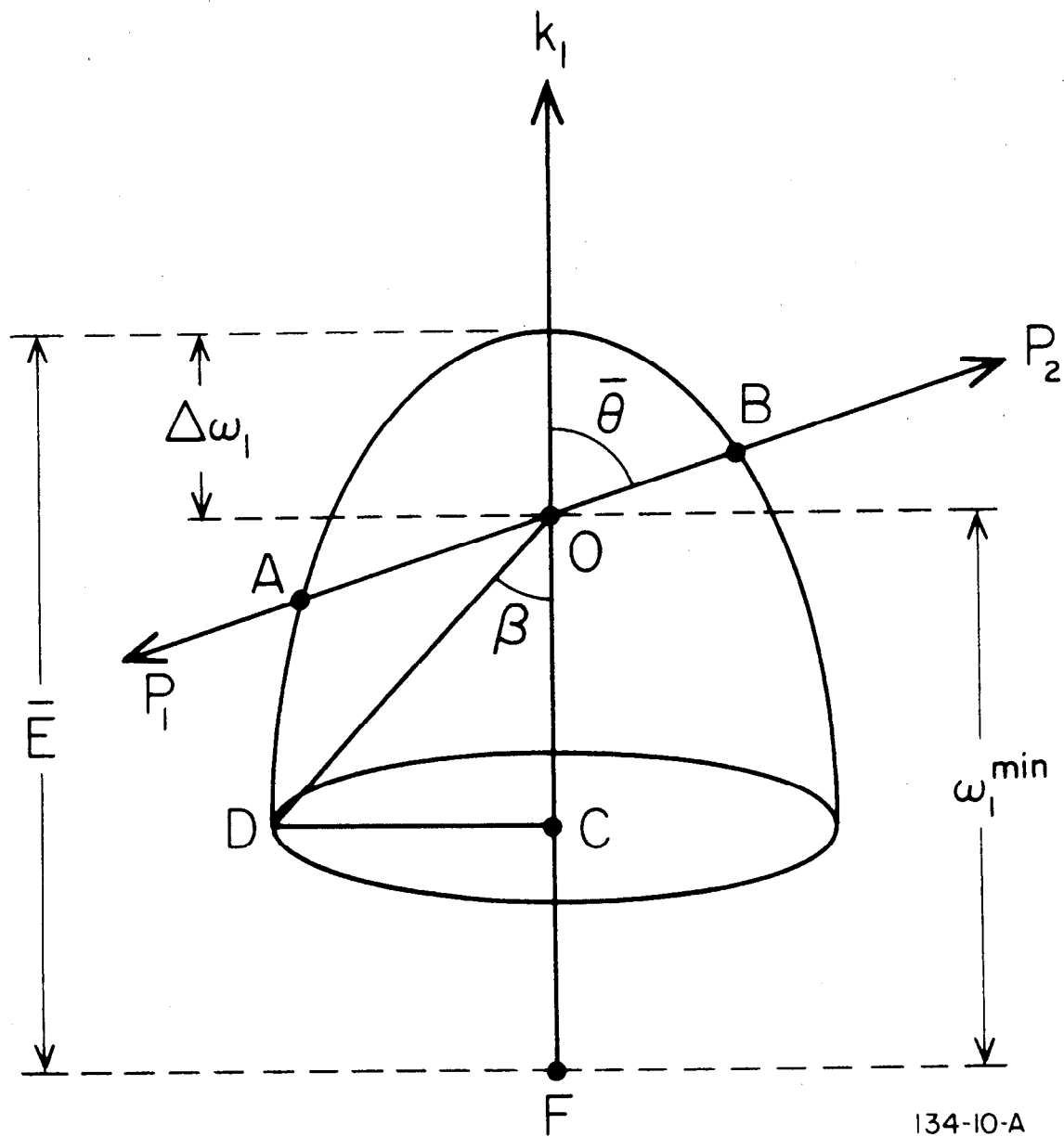
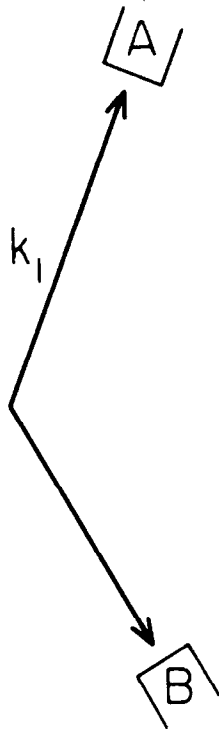
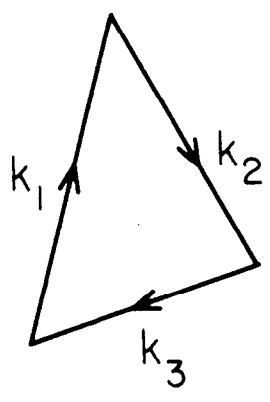


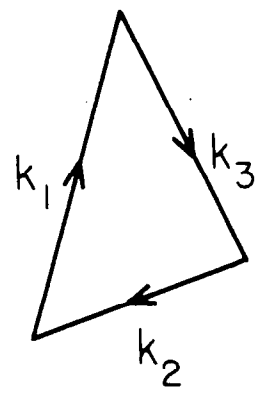
FIGURE 10



( a )



( b )



( c )

134-II-A

FIGURE II